Combinatorial synthesis of novel and potent inhibitors of NADH:ubiquinone oxidoreductase

KC Nicolaou [1,2], JA Pfefferkorn [1], F Schuler [3], AJ Roecker [1], G-Q Cao [1] and JE Casida [3]

Background: NADH:ubiquinone oxidoreductase (complex I) is the first of three large enzyme complexes located in the cell's inner mitochondrial membrane which form the electron transport chain that carries electrons from NADH to molecular oxygen during oxidative phosphorylation. There is significant interest in developing small molecule inhibitors of this enzyme for use as biological probes, insecticides and potential chemopreventive/chemotherapeutic agents. Herein we describe the application of novel natural product-like libraries to the discovery of a family of potent benzopyran-based inhibitors.

Results: Initially a combinatorial library of benzopyrans, modeled after natural products, was synthesized using a solid phase cycloloading strategy. Screening of this diversity oriented library for inhibitory potency against NADH:ubiquinone oxidoreductase activity in vitro using bovine heart electron transport particles provided several lead compounds which were further refined through a series of focused libraries.

Conclusions: Using this combinatorial library approach, a family of potent 2,2-dimethylbenzopyran-based inhibitors was developed with IC_{50} values in the range of 18–55 nM. Cell-based assays revealed that these inhibitors were rather non-cytotoxic in the MCF-7 cell line; however, they were quite cytostatic in a panel of cancer cell lines suggesting their potential as chemotherapeutic/chemopreventive candidates.

[1]Department of Chemistry and The Skaggs Institute for Chemical Biology, The Scripps Research Institute, 10550 North Torrey Pines Road, La Jolla, CA 92037, USA
[2]Department of Chemistry and Biochemistry, University of California, San Diego, 9500 Gilman Drive, La Jolla, CA 92093, USA
[3]Environmental Chemistry and Toxicology Laboratory, Department of Environmental Science, Policy and Management, University of California, Berkeley, 115 Wellman Hall, Berkeley, CA 94720-3112, USA

Correspondence: KC Nicolaou
E-mail: kcn@scripps.edu

Received: **8 August 2000**
Revisions requested: **14 September 2000**
Revisions received: **6 October 2000**
Accepted: **9 October 2000**

Published: **1 November 2000**

Chemistry & Biology 2000, **7**:979–992

1074-5521/00/$ – see front matter

PII: S1074-5521(00)00047-8

Introduction

NADH:ubiquinone oxidoreductase (complex I) is the first of three large enzyme complexes located in the inner mitochondrial membrane which form the electron transport chain that carries electrons from NADH to molecular oxygen during oxidative phosphorylation (Figure 1) [1]. Complex I is the most intricate enzyme known, consisting of over 40 individual protein sub-units with one non-covalently bound flavin mononucleotide and at least five iron–sulfur clusters. This enzyme serves an essential role

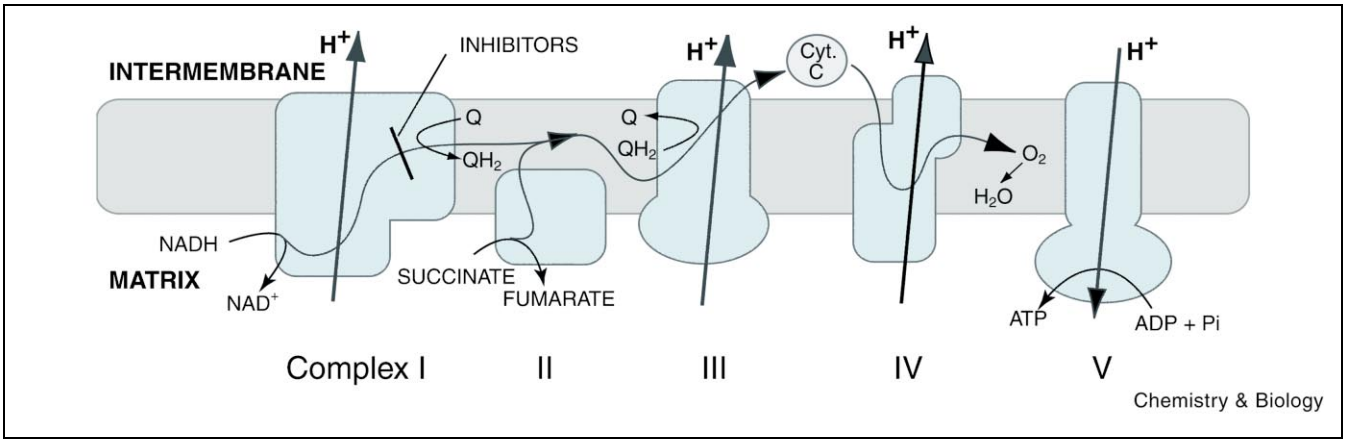

Figure 1. Role of NADH:ubiquinone oxidoreductase (complex I) on oxidative phosphorylation.

in cellular physiology such that structural or functional deficiencies in it have been implicated in the pathogenesis of diseases such as Parkinson's, focal dystonia and Leber's hereditary optic neuropathy [2].

A variety of natural and synthetic inhibitors of complex I (see representative examples in Figure 2) have found multiple applications [3]. First, inhibitors have been used to elucidate the role of this enzyme in normal cell physiology and also to mimic complex I deficiencies in order to study mitochondrial diseases [4]. Second, the structure–activity relationships (SAR) developed using inhibitors have provided important insights into the functional architecture of this complicated enzyme system; furthermore, affinity probes, constructed based upon these inhibitors, have proven valuable in identifying and characterizing the components of complex I [5–7]. Third, NADH:ubiquinone oxidoreductase continues to be a preferred target for the development of commercial insecticides and acaricides [8]. Fourth, and more recently, it has been demonstrated that inhibition of NADH:ubiquinone oxidoreductase causes a corresponding reduction in the activity of ornithine decarboxylase (ODC), possibly through interruption of signal transduction pathways [9]. ODC is responsible for the biosynthesis of polyamine growth factors required for normal cellular proliferation [10]. Since the overexpression of ODC activity in tumor cells contributes to aberrant proliferation, the ability of complex I inhibitors to reduce ODC activity makes them potential candidates for development as chemotherapeutic and/or chemopreventive

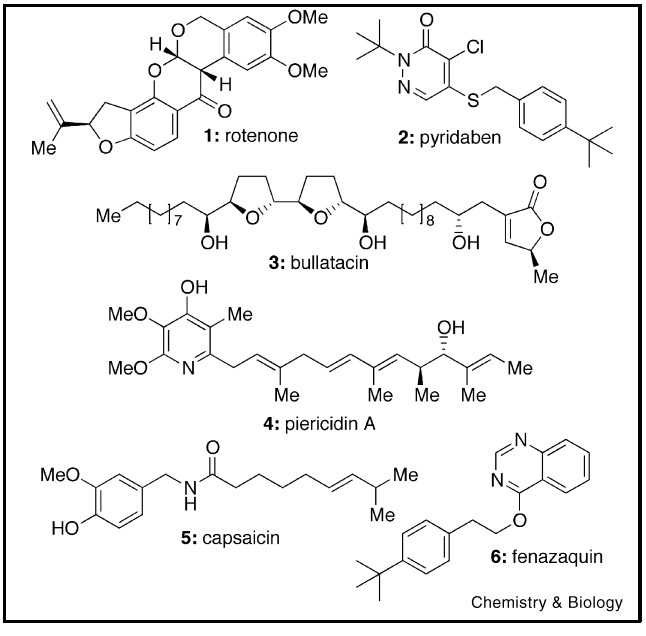

Figure 2. Representative natural and synthetic inhibitors of NADH:ubiquinone oxidoreductase.

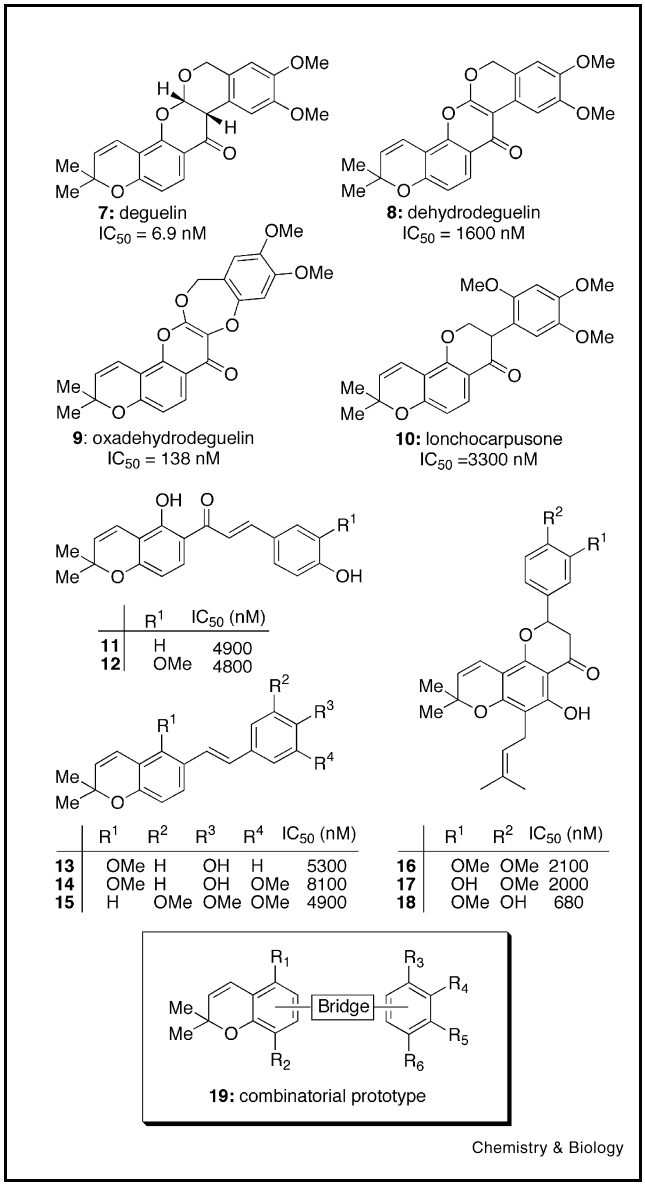

Figure 3. Selected natural product inhibitors (**7**–**18**) of NADH:ubiquinone oxidoreductase isolated from Cubé resin and combinatorial library prototype (**19**).

agents [11–13]. Moreover, there is increasing evidence that modulation of complex I activity, through small molecules, can induce apoptosis thus further supporting the potential of these inhibitors as anticancer agents [14].

The goal of this study was to identify novel lead compounds through the screening of natural product-like combinatorial libraries. The motivation stemmed from the previous characterization of a family of naturally occurring inhibitors isolated from Cubé resin, an extract of the roots of *Lonchocarpus utilis* and *Lonchocarpus urucu*, which has been used as a botanical insecticide for decades [15,16].

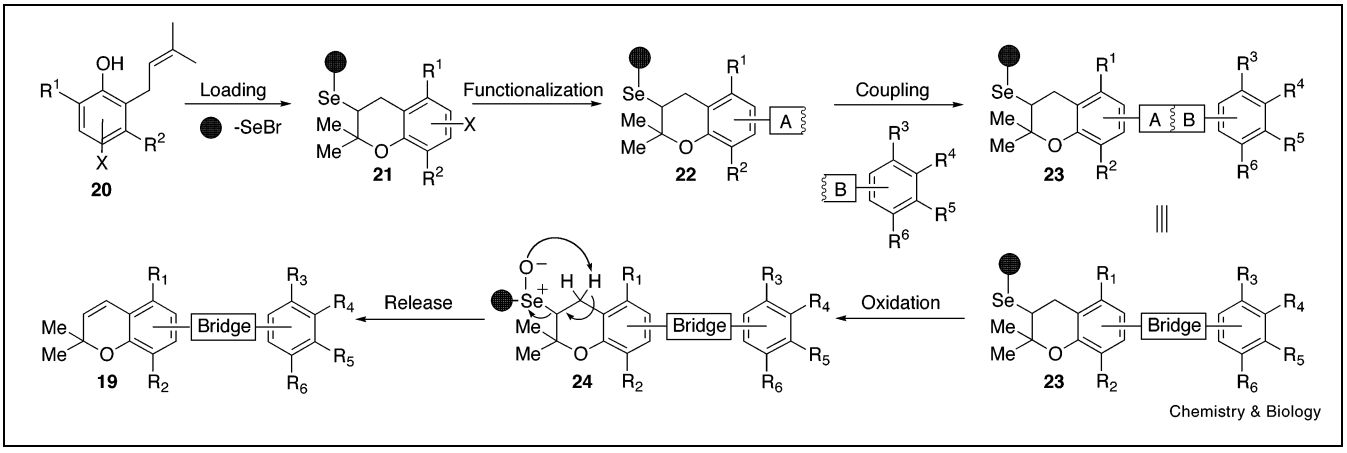

Scheme 1. General strategy for the solid phase combinatorial synthesis of natural product-like small molecules as potential inhibitors of NADH:ubiquinone oxidoreductase. *o*-Prenylated phenols are cycloloaded onto a polystyrene-based selenenyl bromide resin to provide immobilized benzopyran scaffolds which are functionalized and then coupled to a second aromatic unit, thereby affording bridged structures **23**. Library members are released from the resin by oxidation of the selenium moiety to the corresponding selenoxide which undergoes spontaneous *syn*-elimination to afford the desired benzopyran systems (**19**).

Separation of the constituents of this resin provided the major components rotenone (**1**, Figure 2) and deguelin (**7**, Figure 3) along with minor constituents, including dehydrodeguelin (**8**), oxadehydrodeguelin (**9**), lonchocarpusone (**10**), 4-hydroxylonchocarpene (**11**), 4-hydroxy-3-methoxylonchocarpene (**12**), stilbenes **13–15** and isoflavones **16–18** (Figure 3) among others. Inspection of natural products **7–18** revealed an interesting homology as all possessed a 2,2-dimethylbenzopyran motif linked to a terminal aromatic ring through a variety of molecular bridges. De-

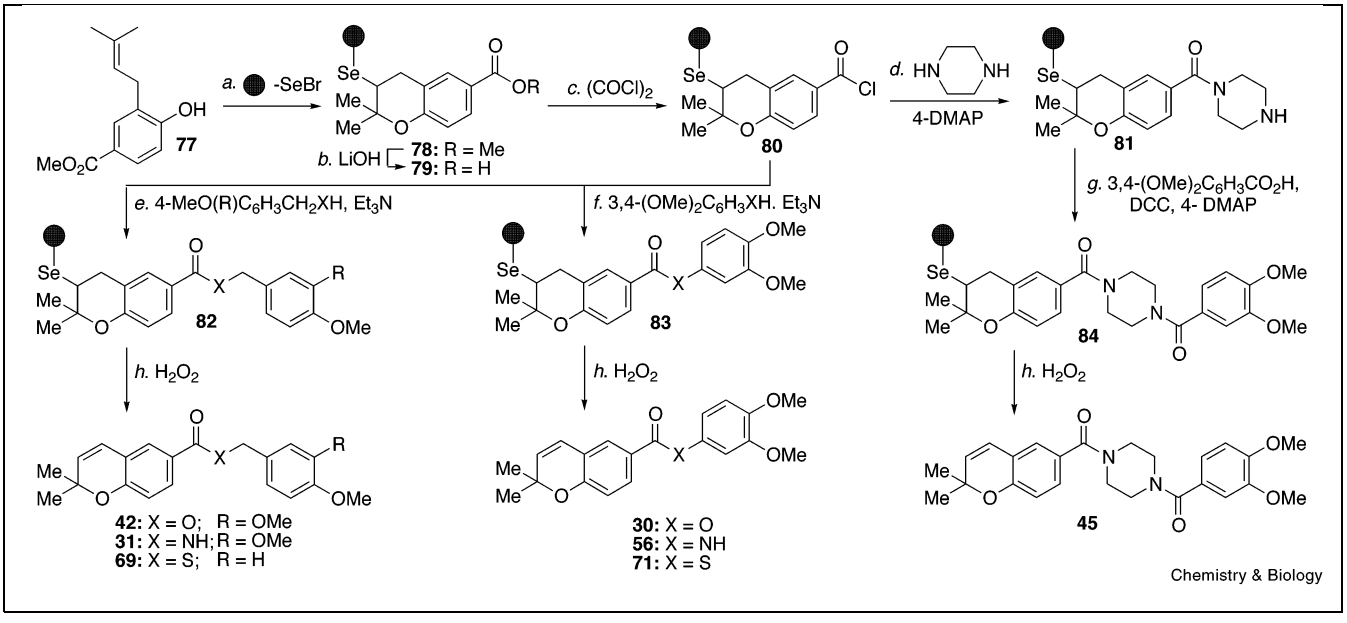

Scheme 2. Representative procedures for the solid phase synthesis of amides, esters, and thioesters. Reagents and conditions: **(a)** 0.5 equivalent (equiv) of selenenyl bromide resin (1.1 mmol/g), CH_2Cl_2, 25°C, 20 min; **(b)** 10.0 equiv of LiOH, THF:H_2O (20:1), 50°C, 48 h; **(c)** 10.0 equiv of $(COCl)_2$, cat. DMF, CH_2Cl_2, 40°C, 2 h; **(d)** 10.0 equiv of piperazine, 1.0 equiv of 4-DMAP, CH_2Cl_2, 25°C, 12 h; **(e)** 5.0 equiv of 3,4-$(OMe)_2C_6H_3CH_2XH$ (X = O, NH, S), 15.0 equiv of Et_3N, 1.0 equiv of 4-DMAP, CH_2Cl_2, 25°C, 12 h; **(f)** 5.0 equiv of 3,4-$(OMe)_2C_6H_3XH$ (X = O, NH, S), 15.0 equiv of Et_3N, 1.0 equiv of 4-DMAP, CH_2Cl_2, 25°C, 12 h; **(g)** 5.0 equiv of 3,4-$(OMe)_2C_6H_3CO_2H$, 5.0 equiv of DCC, 1.0 equiv of 4-DMAP, CH_2Cl_2, 25°C, 24 h; **(h)** 6.0 equiv of H_2O_2, THF, 25°C, 20 min. DCC = 1,3-dicyclohexylcarbodiimide, 4-DMAP = 4-(dimethylamino)pyridine, DMF = *N,N*-dimethylformamide.

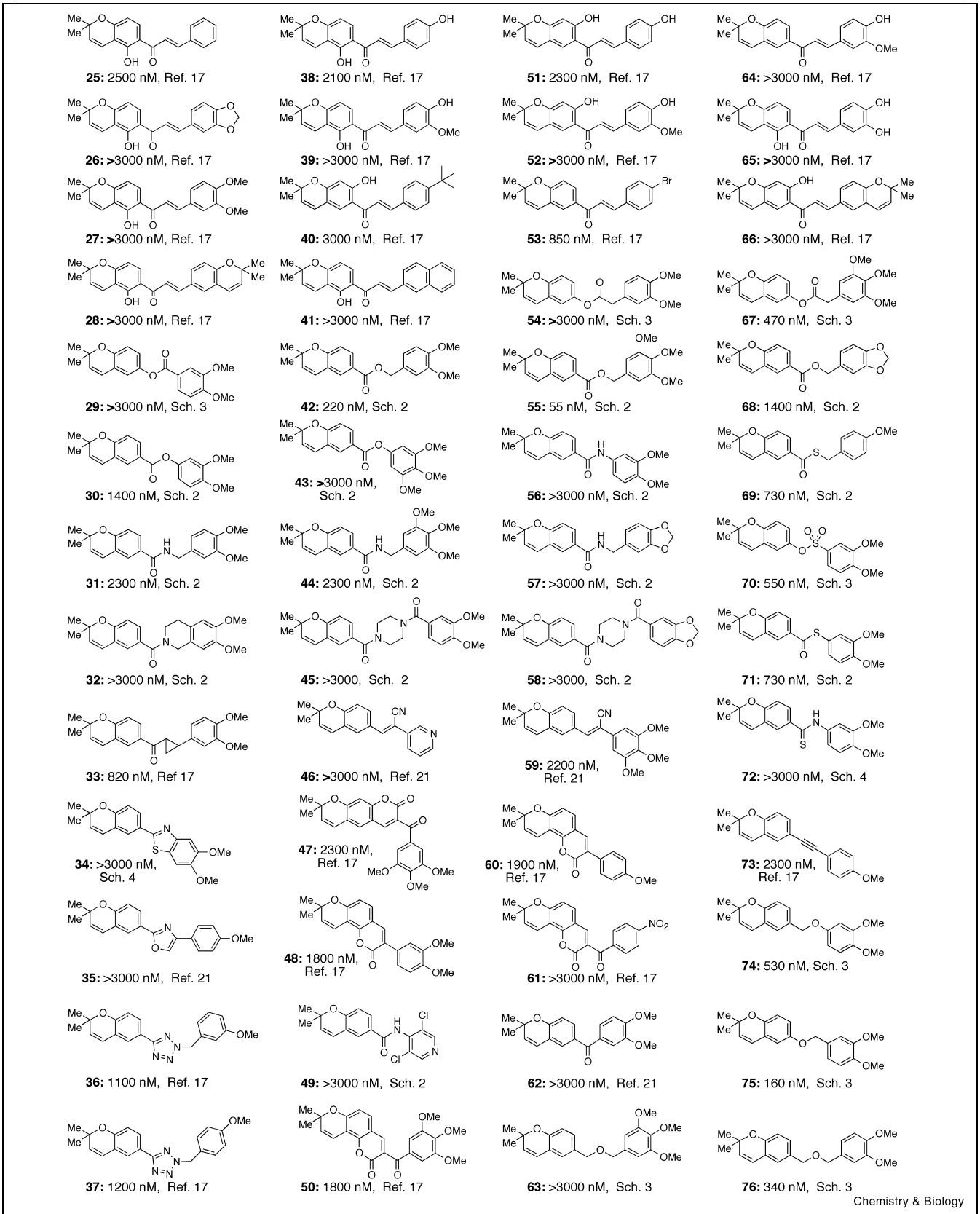

Figure 4. Structures and IC_{50} values of screening library. The synthesis of individual members is described in the schemes and references indicated.

spite the diversity in these bridging units, all of the compounds (**7–18**) inhibited complex I activity in in vitro assays [15,16]. Not surprisingly however, the potency of inhibition was strongly influenced by the orientation through which the 'bridge' unit positioned the two ring systems with respect to each other. For example, deguelin (IC_{50} = 6.9 nM) is almost 500-fold more active than lonchocarpusone (IC_{50} = 3300 nM). Given this effect, it was envisioned that screening a benzopyran-based combinatorial library wherein this 'bridge' unit was varied (i.e. structure **19**, Figure 3) might lead to the identification of interesting SAR, and potentially to new lead compounds in this series. Notably, it was anticipated that these lead compounds, synthesized through combinatorial chemistry, would be more amenable (as compared to the parent natural products) to further synthetic modifications as required for optimization of physical and pharmacological properties.

Results and discussion

First generation discovery library: the bridge region III (compounds 25–76)

Having recently completed the synthesis of several large benzopyran-based combinatorial libraries, we were well positioned to assemble a suitable, first generation library for evaluating this hypothesis [17–19]. Thus, a 52-membered library was selected for preliminary screening as shown in Figure 4. Members were selected so as to simultaneously evaluate both the nature of the 'bridge' unit as well as the importance of substituents on the terminal aromatic ring system. Most members of this discovery library had been previously synthesized via a selenium-based, solid phase strategy as outlined in Scheme 1. In this approach, a series of *ortho*-prenylated phenols (**20**) were cycloloaded (through a six-*endo*-trig electrophilic cyclization reaction) onto a polystyrene-based selenenyl bromide resin to afford resin-bound benzopyran scaffolds (**21**) [20,21]. These scaffolds were then functionalized and coupled with a second aromatic unit so as to create diverse bridge types (**23**). Upon completion, structures of type **23** could be further derivatized if necessary, and then released from the solid support by oxidation of the selenoether to the corresponding selenoxide which could undergo facile *syn*-elimination. The synthesis of compounds **25–28**, **33**, **35–41**, **46–48**, **50–54**, **59–62**, **64–66** and **73** (Figure 4) via this solid phase route has been described previously [17–21]. Representative procedures for the solid phase synthesis of the remaining members of the described library are illustrated in Scheme 2–4. All library members for biological assay were chromatographically and spectroscopically (^{1}H-nuclear magnetic resonance) homogeneous.

As shown in Scheme 2, the first type of library members to be constructed was a series of acyl derivatives. Initially, *ortho*-prenylated phenol **77** was cycloloaded onto a selenenyl bromide resin [22] to afford benzopyran scaffold **78**. The methyl ester of **78** was then hydrolyzed (LiOH, THF:H_2O, 40°C) to the corresponding carboxylic acid which was converted to acid chloride **80** by treatment with oxalyl chloride in the presence of catalytic amounts of *N*,*N*-dimethylformamide (DMF). This acid chloride then participated in three parallel reaction pathways. In the first sequence, treatment of acid chloride **80** with piperazine and 4-(dimethylamino)pyridine (4-DMAP) provided amide **81**. The secondary amine of structure **81** was then coupled to 3,4-dimethoxybenzoic acid in the presence of 1,3-dicyclohexylcarbodiimide (DCC) and 4-DMAP to provide diamide **84** which was released from the solid support by treatment with H_2O_2, giving diamide **45**. In the second pathway, acid chloride **80** was treated (in parallel) with a series of aryl nucleophiles including 3,4-dimethoxyphenol, 3,4-dimethoxyaniline and 3,4-dimethoxythiophenol to provide structures of type **83**, which upon oxidative cleavage afforded ester **30**, amide **56** and thioester **71**, respectively. In the last pathway, acid chloride **80** was reacted with a series of benzylic nucleophiles including 3,4-dimethoxybenzyl alcohol, 3,4-dimethoxybenzyl amine and 4-methoxy-α-toluene thiol to provide structures of type **82** which were oxidatively cleaved to afford ester **42**, amide **31** and thioester **69**, respectively. In addition to the representative compounds shown here, this procedure

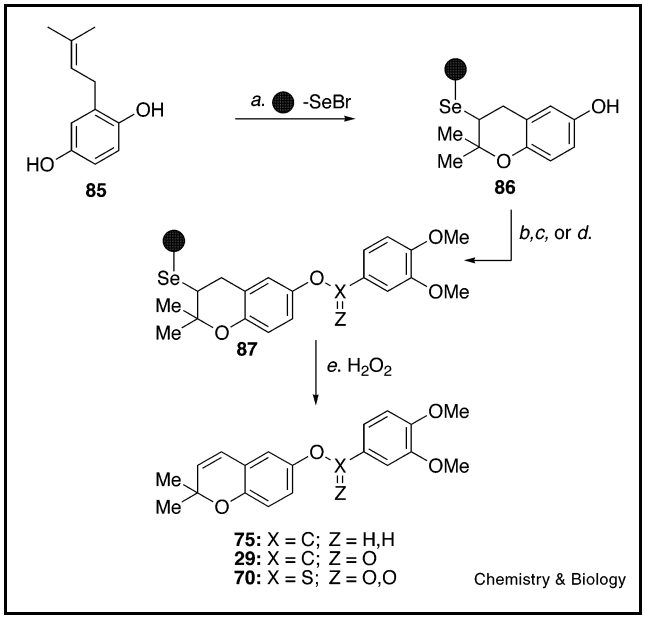

Scheme 3. Representative procedures for the solid phase synthesis of ether (**75**), ester (**29**), and sulfonate (**70**) compounds. Reagents and conditions: **(a)** 0.5 equiv of selenenyl bromide resin (1.1 mmol/g), CH_2Cl_2, 25°C, 20 min; **(b)** 5.0 equiv of 3,4-dimethoxybenzyl chloride, 5.0 equiv of K_2CO_3, DMF, 60°C, 12 h; **(c)** 5.0 equiv of 3,4-dimethoxybenzoic acid, 5.0 equiv of DCC, 1.0 equiv of 4-DMAP, CH_2Cl_2, 25°C, 24 h; **(d)** 5.0 equiv of 3,4-dimethoxybenzenesulfonyl chloride, 10.0 equiv of Et_3N, 1.0 equiv of 4-DMAP, CH_2Cl_2, 25°C, 12 h; **(e)** 6.0 equiv of H_2O_2, THF, 25°C, 20 min.

was repeated in an analogous and parallel manner to prepare compounds **32**, **43–44**, **49**, **55**, **57–58** and **68–69** (Figure 4).

As shown in Scheme 3, additional library members with other types of bridging units were constructed from a phenolic benzopyran system. Initially, resin-bound phenol **86** was prepared through the cycloloading of prenylated hydroquinone **85**. Library members containing an ether-type bridge were then constructed by alkylation of **86** with 3,4-dimethoxylbenzyl chloride in the presence of K_2CO_3 followed by oxidative cleavage to afford ether **75**. Ester derivatives were constructed by acylation of phenol **86** with 3,4-dimethoxybenzoic acid, DCC and 4-DMAP to afford, after oxidative cleavage, ester **29**. Lastly, sulfonate derivatives were constructed by treatment of phenol **86** with 3,4-dimethoxybenzenesulfonyl chloride, Et_3N, and 4-DMAP followed by oxidative cleavage to afford sulfonate **70**. In addition to the representative compounds shown here, this procedure was also repeated in an analogous and parallel manner to prepare compounds **63**, **67**, **74** and **76** (Figure 4).

As shown in Scheme 4, several sulfur-containing library members were synthesized through a halogen–metal exchange reaction. Initially, prenylated bromophenol **88** was cycloloaded onto the selenenyl bromide resin to give benzopyran **89**. Aryl bromide **89** was subjected to a halogen–metal exchange reaction by treatment with *n*-BuLi at −78°C and then warming to 0°C over 2 h at which time 3,4-dimethoxyphenylisothiocyanate was added. Cleavage of the supposed thioamide **90** by treatment with H_2O_2 unexpectedly afforded a separable mixture of thioamide **72** and thiazole **34** the latter being presumably formed as a result of excess base present in the halogen–metal exchange reaction.

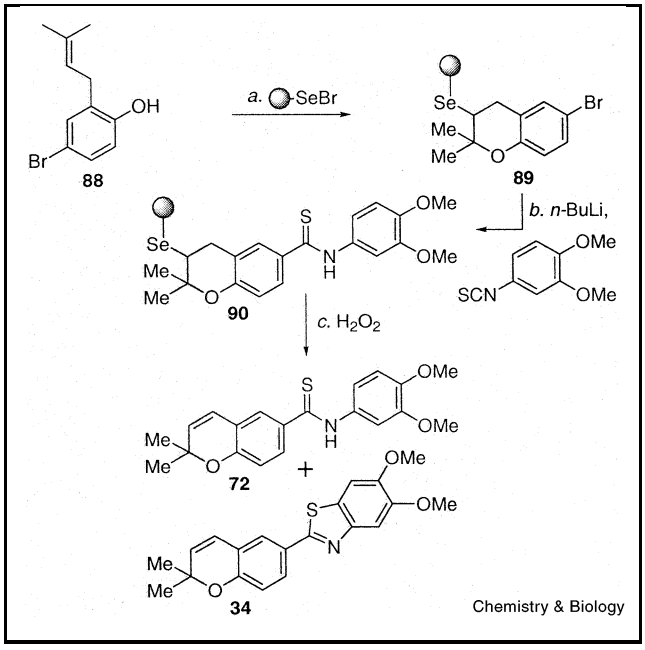

Scheme 4. Solid phase synthesis of thioamide (**72**) and thiazole (**34**) systems. Reagents and conditions: **(a)** 0.5 equiv of selenenyl bromide resin (1.1 mmol/g), CH_2Cl_2, 25°C, 20 min; **(b)** 10.0 equiv of *n*-BuLi (1.6 M in hexanes), THF, −78→0°C, 2 h; then 10.0 equiv of 3,4-dimethoxyphenylisothiocyanate, THF, −78→25°C, 1 h; **(c)** 6.0 equiv of H_2O_2, THF, 25°C, 20 min.

Table 1
Summary of biological data from evaluation of first generation library and proposed lead structures.

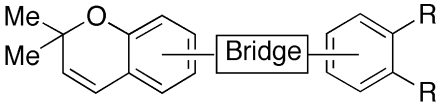

Bridge	IC_{50} (nM)	Bridge	IC_{50} (nM)
Chalcone	850–(>3000)	Alkyne	2300
Stilbene	2200–(>3000)	Ester	55–(>3000)
Coumarin	1900–(>3000)	Amide	2300–(>3000)
Heterocycle	1100–(>3000)	Ether	160–800

First generation lead compounds

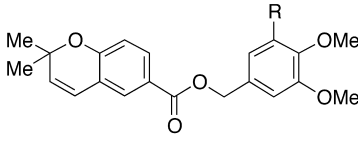

	R	IC_{50} (nM)
42	H	220
55	OMe	55

Strategic regions for SAR optimization

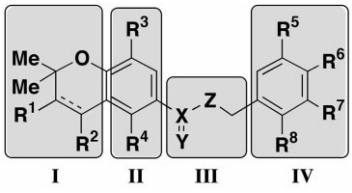

This primary library was screened for inhibitory potency against NADH:ubiquinone oxidoreductase activity as described below. This screening revealed several structure–activity trends (summarized in Table 1 and discussed in detail in the SAR section) which ultimately provided esters **42** and **55** as lead compounds. As described below, a series of focused libraries were then synthesized using a combination of solid and solution phase chemistry in an attempt to evaluate particular structural sub-regions (denoted **I–IV** in Table 1) of the lead structure, thus allowing SAR to be developed.

First focused library, aryl substituents, regions II and IV (compounds 91–127)

The first of these follow-up libraries focused on regions **II** and **IV** of the lead structure. Of particular interest was how

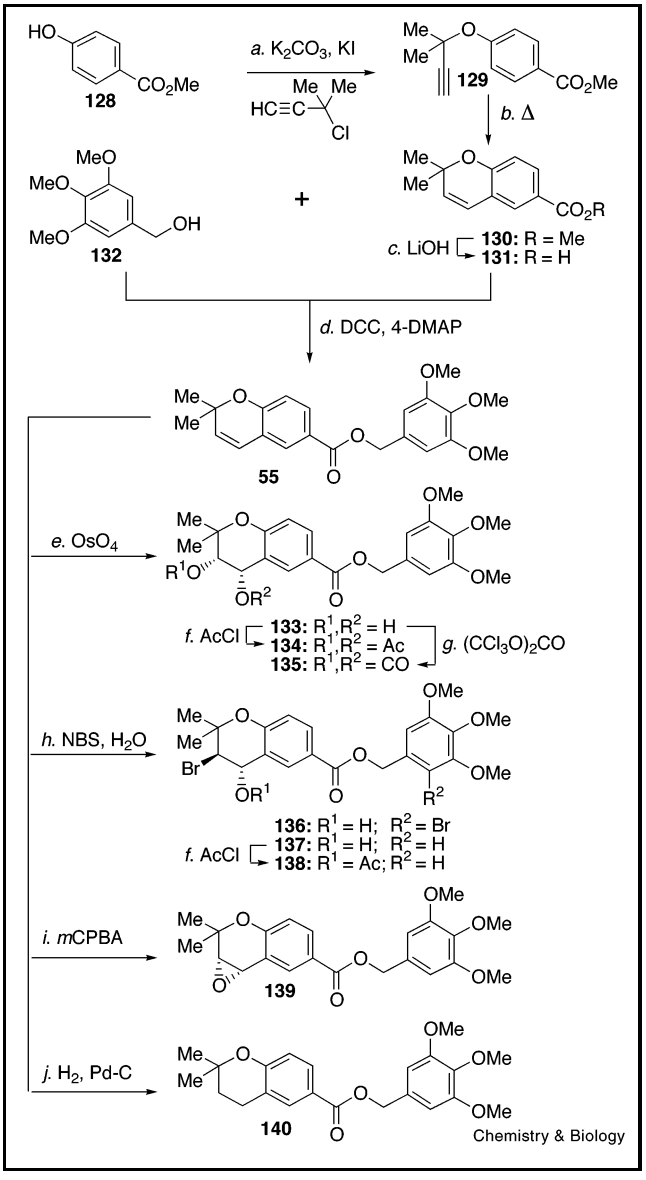

Scheme 5. Solution phase synthesis of 3,4,5-trimethoxybenzyl ester (**55**) and modified pyran analogs and their biological activities. Reagents and conditions: **(a)** 2.0 equiv of 3-chloro-3-methyl-1-butyne, 2.0 equiv of K_2CO_2, 1.7 equiv of KI, 0.02 equiv of CuI, DMF, 65°C, 3 h, 88%; **(b)** Et_2NPh, 195°C, 1 h, 100%; **(c)** 2.0 equiv of LiOH, THF:H_2O (10:1), 40°C, 12 h, 95%; **(d)** 1.1 equiv of 3,4,5-trimethoxybenzyl alcohol, 1.2 equiv of DCC, 0.1 equiv of 4-DMAP, CH_2Cl_2, 25°C, 12 h, 89%; **(e)** 0.1 equiv of OsO_4, 1.1 equiv of NMO, *t*-BuOH:THF:H_2O (10:3:1), 25°C, 2 h, 71%; **(f)** 3.0 equiv of AcCl, 5.0 equiv of pyridine, CH_2Cl_2, 0→25°C, 1 h, 97%; **(g)** 5.0 equiv of triphosgene, 10.0 equiv of pyridine, CH_2Cl_2, 0°C, 1 h, 80%; **(h)** 1.1 equiv of NBS, DMSO:H_2O (10:1), 0°C, 1 h, 80%; **(i)** 1.0 equiv of *m*-CPBA, 3.0 equiv of Na_2CO_3, CH_2Cl_2, 25°C, 24 h, 69%; **(j)** 0.2 equiv of 10% Pd-C, H_2, MeOH:hexane (1:1), 25°C, 6 h, 96%. DMSO = methyl sulfoxide, NMO = 4-methylmorpholine *N*-oxide, NBS = *N*-bromosuccinimide, *m*-CPBA = *m*-chloroperoxybenzoic acid. Compounds **133**–**139** were synthesized and assayed as racimates with the relative stereochemistry as shown.

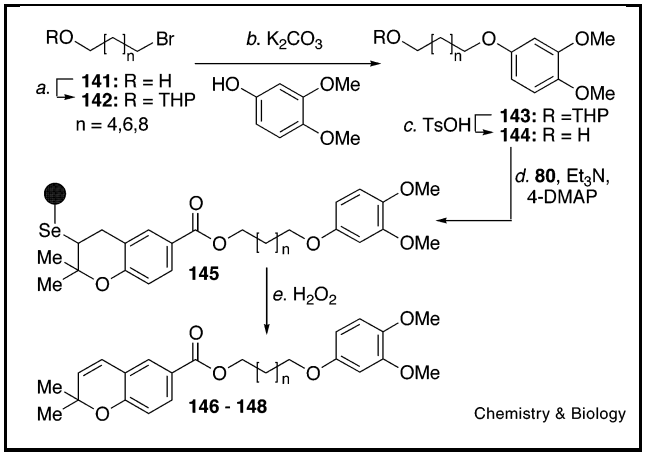

Scheme 6. Synthesis of long chain 3,4-dimethoxyphenyl esters. Reagents and conditions: **(a)** 1.5 equiv of 3,4-dihydropyran, 0.1 equiv of PPTS, CH_2Cl_2, 25°C, 2 h; **(b)** 2.0 equiv of 3,4-dimethoxyphenol, 2.0 equiv of K_2CO_3, acetone, 40°C, 12 h; **(c)** 1.2 equiv of TsOH·H_2O, THF:MeOH (9:1), 25°C, 1 h; **(d)** 0.5 equiv of **80**, 10.0 equiv of Et_3N, 1.0 equiv of 4-DMAP, CH_2Cl_2, 25°C, 12 h; **(e)** 6.0 equiv of H_2O_2, THF, 25°C, 20 min.

substituent patterns on these two aromatic systems would effect inhibitory activity. Hence, a series of esters (**91**–**127**, Figure 5) were synthesized in parallel on solid support using an identical protocol to that described in Scheme 2. The aromatic building blocks employed contained a variety of substituents including alkyl groups, halogens, alkoxy groups, hydroxyl groups, alcohols and nitro groups in order to assess both steric and electronic effects.

Second focused library, dimethylpyran modifications, region I (compounds 133–140)

The synthesis of the second of the follow-up libraries relied upon solution phase chemistry and was designed so as to evaluate how modifications in the pyran ring system might effect biological activity. Thus, as shown in Scheme 5, lead ester **55** was first resynthesized on a large scale from 4-hydroxymethyl benzoate **128** by initial *O*-alkylation with 3-chloro-3-methyl-1-butyne to give ether **129** [23]. Heating of alkyne **129** in *N*,*N*-diethylaniline at 195°C for 1 h induced an aromatic Claisen rearrangement to provide benzopyran **130** in quantitative yield [23]. The methyl ester of **130** was hydrolyzed (LiOH, THF:H_2O, 40°C, 12 h) to the free acid **131** which was coupled to 3,4,5-trimethoxybenzyl alcohol in the presence of DCC and 4-DMAP to furnish ester **55**. With the ester **55** in hand, several derivatization reactions were employed to provide the series of pyran-modified analogs **133**–**140**. First, the olefin of ester **55** was dihydroxylated [24] (cat OsO_4, NMO, *t*-BuOH:THF:H_2O, 25°C, 6 h) to afford diol **133** which was subsequently acetylated to diacetate **134** and reacted with triphosgene to provide carbonate **135**. In a second event, ester **55** was treated [25] with NBS in the presence

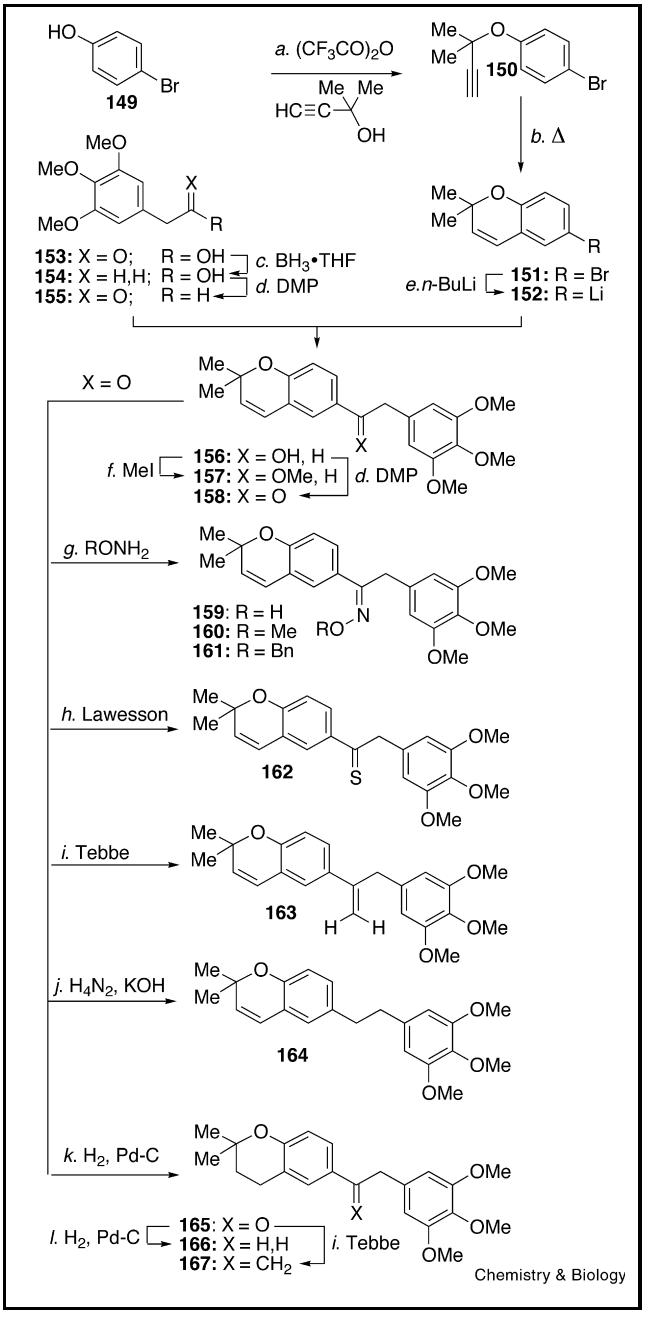

Scheme 7. Solution phase synthesis of 3,4,5-trimethoxyphenylketone (**158**) and analogs thereof. Reagents and conditions: **(a)** 1.2 equiv of 2-methyl-3-butyn-2-ol, 1.2 equiv of trifluoroacetic anhydride, 1.5 equiv of DBU, MeCN, 0°C, 6 h, 100%; **(b)** Et_2NPh, 195°C, 1 h, 100%; **(c)** 3.0 equiv of BH_3·THF, THF, 0→25°C, 2 h, 100%; **(d)** 1.1 equiv of Dess–Martin periodinane, CH_2Cl_2, 25°C, 1 h, 90%; **(e)** 1.1 equiv of *n*-BuLi (1.6 M in hexanes), THF, −78°C, 15 min; then 2.0 equiv of **155**, THF, −78°C, 15 min, 45%; **(f)** 5.0 equiv of MeI, 2.0 equiv of NaH, THF, 0→25°C, 12 h, 85%; **(g)** 4.0 equiv of $RONH_2$ (R = H, Me, Bn), 5.0 equiv of K_2CO_3, EtOH, 75°C, 2 h, R = H: 52%, R = Me: 78%, R = Bn: 81%; **(h)** 3.0 equiv of Lawesson's reagent, toluene, 100°C, 3 h, 42%; **(i)** 1.2 equiv of Tebbe reagent, THF, −40→0°C, 30 min, 88%; **(j)** 10.0 equiv of H_4N_2·H_2O, 10.0 equiv of KOH, di(ethylene glycol), 245°C, 6 h, 21%; **(k)** 0.2 equiv of 10% Pd-C, H_2, MeOH:hexane (1:1), 25°C, 6 h; **(l)** 2.0 equiv of 10% Pd-C, H_2, MeOH, 25°C, 12 h.
←

Third focused library, the bridge region III (compounds 146–179)

A final library in this series sought to further investigate the nature of the bridge unit. Of particular interest was the effect of length, structure and polarity of this bridge as illustrated in Scheme 6–9. In order to access the relationship between bridge length and biological activity, a set of longer chain analogs **146–148** was synthesized as illustrated in Scheme 6 where alcohols of type **141** were prepared by alkylation of the corresponding bromoalcohols and then coupled to resin-bound acid chloride **80** as previously described. Subsequently, we sought to determine whether or not an ester functionality was optimal as a bridge unit. This was accomplished by the solution phase synthesis of vari-

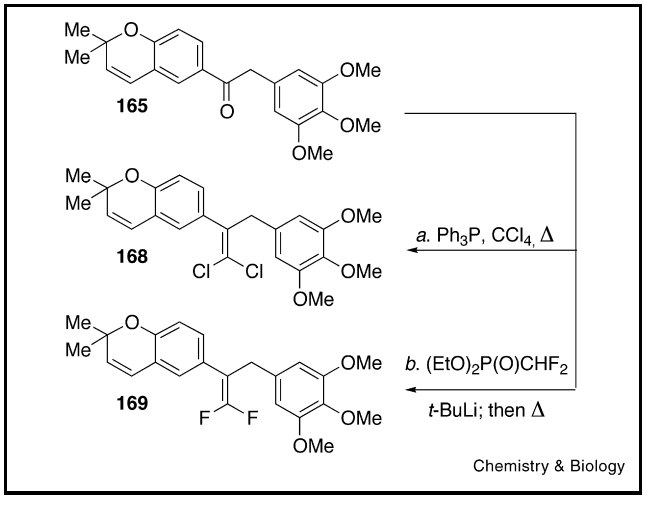

Scheme 8. Solution phase synthesis of difluoro- and dichlorostyrene analogs **168** and **169**. Reagents and conditions: **(a)** 2.0 equiv of Ph_3P, CCl_4, 60°C, 15 h, 60%; **(b)** 5.0 equiv of $(EtO)_2P(O)CHF_2$, 4.0 equiv of *t*-BuLi, DME, −78°C, 1 h; then 85°C, 15 h, 20%.

of H_2O to provide a mixture of bromohydrins **136** and **137** as a result of partial bromination of the terminal aromatic ring (i.e. structure **136**). Bromohydrin **137** was subsequently acetylated (AcCl, pyridine, CH_2Cl_2, 25°C, 1 h) to afford acetate **138**. Additionally, ester **55** was converted to the corresponding epoxide **139** by treatment with *m*-CPBA [26]. Finally, the olefin of ester **55** was saturated by hydrogenation over 10% Pd–C to provide the corresponding saturated pyran system **140**.

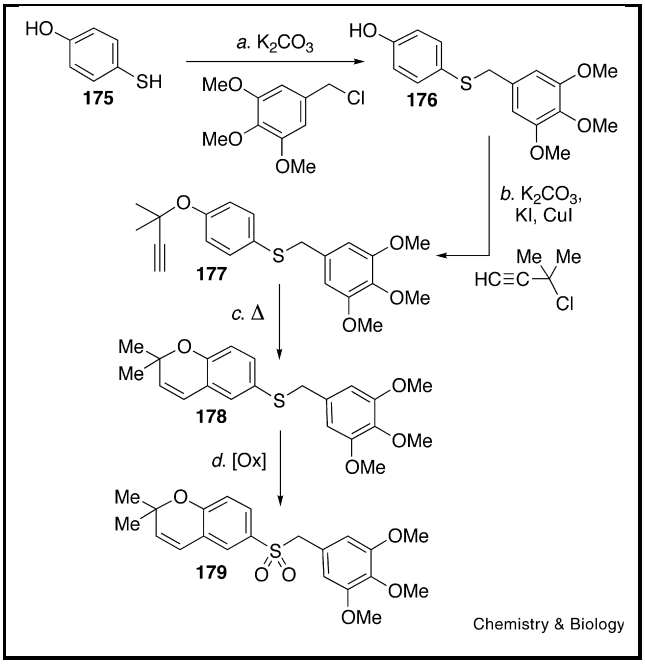

Scheme 9. Synthesis of 3,4,5-trimethoxyphenylthioether **178** and 3,4,5-trimethoxyphenylsulfone **179**. Reagents and conditions: **(a)** 1.0 equiv of 3,4,5-trimethoxybenzyl chloride, 3.0 equiv of K_2CO_3, 0.2 equiv of TBAI, DMF, 25°C, 2 h, 74%; **(b)** 2.0 equiv of 3-chloro-3-methyl-1-butyne, 2.0 equiv of K_2CO_3, 1.7 equiv of KI, 0.02 equiv of CuI, DMF, 65°C, 3 h, 40%; **(c)** Et_2NPh, 195°C, 1 h, 100%; **(d)** 2.5 equiv of OXONE, 2.5 equiv of $NaHCO_3$, THF:H_2O (2:1), 25%. TBAI = tetrabutylammonium iodide.

ous other linking units, including ketones, oximes, thioketones, alkyl chains, thioethers and sulfones as shown in Schemes 7–9. As illustrated in Scheme 7, various keto analogs and their derivatives were constructed starting from 4-bromophenol **149**. Following the procedure of Ding, 4-bromophenol (**149**) was alkylated with the in situ generated triflate of 2-methyl-3-butyn-2-ol to afford **150**, which was heated to 195°C in *N*,*N*-dimethylaniline inducing an aromatic Claisen rearrangement and providing benzopyran **151** in quantitative yield [27]. Subsequent treatment of **151** with *n*-BuLi afforded aryl lithium **152**, which was immediately quenched by addition of aldehyde **155** (synthesized from phenylacetic acid **153**, as indicated in Scheme 7) to provide benzyl alcohol **156**. Dess–Martin periodinane oxidation of alcohol **156** afforded ketone **158**. Incidentally, the methyl ether analog of alcohol **156**, compound **157**, was also synthesized from alcohol **156** via alkylation with MeI in the presence of NaH. With ketone **158** available, a series of modified keto-analogs were then constructed. Thus, oximes **159–161** were prepared by condensation of ketone **158** with the appropriate hydroxy or alkoxy amines in the presence of K_2CO_3. Thioketone **162** was prepared by reaction of ketone **158** with Lawesson's reagent in toluene at 100°C for 3 h, whereas the corresponding olefin analog **163** was constructed by treatment of ketone **158** with Tebbe reagent. Wolf–Kishner reduction of **158** (H_4N_2, KOH, ·) afforded the alkyl variant **164**, while hydrogenation over 10% Pd–C provided the saturated version (i.e. **165**) of ketone **158** as well as of analogs **163** and **164** (i.e. **167** and **166**, respectively). Additional variations of ketone **158** were also constructed to address the importance of tether length and bridge substitution. These analogs were synthesized via an analogous protocol to that shown in Scheme 7 and their structures (**170–174**) are illustrated in Figure 5.

Several halogenated derivatives of styrene **163** were also prepared as illustrated in Scheme 8. Hence, ketone **165** was treated with Ph_3P in CCl_4 at 60°C to afford dichloro-analog **168** [28]. Additionally, ketone **165** was added to a solution of diethyl(difluoromethyl)phosphonate and *t*-BuLi in DME at −78°C and then warmed to 25°C,

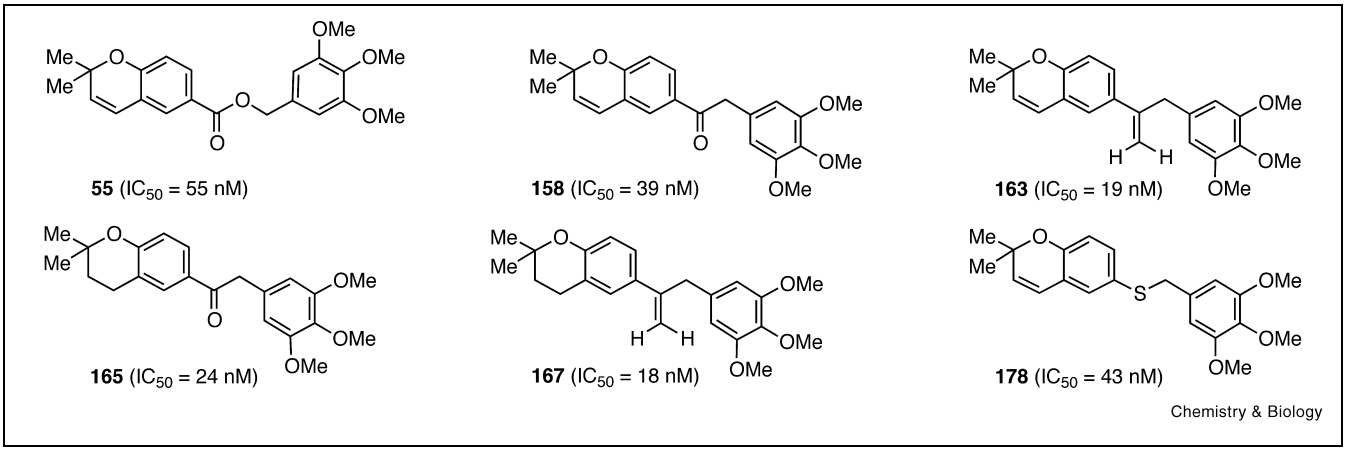

Figure 6. Lead compounds (and their IC_{50} values) selected for evaluation in cell-based assays.

and finally to 85°C to ultimately afford difluoro-analog **169** [29].

A final set of compounds for addressing the nature of the bridge unit was prepared as illustrated in Scheme 9 in an attempt to optimize the activity observed for ether **75** during screening of the first generation library. The thioether variant of this analog was prepared from 4-mercaptophenol (**175**) by selective *S*-alkylation with 3,4,5-trimethoxybenzyl chloride and K_2CO_3 to provide thioether **176** [30]. Subsequent *O*-alkylation was effected with 3-chloro-3-methyl-1-butyne to give alkynyl ether **177**. Heating of alkyne **177** in *N*,*N*-diethylaniline at 195°C for 1 h induced an aromatic Claisen rearrangement furnishing benzopyran **178** in quantitative yield. A portion of thioether **178** was then oxidized with OXONE® to afford the corresponding sulfone **179**.

SAR

SAR optimization was carried out on each of the four regions (**I–IV**) of interest guided by the inhibitory potency for NADH:ubiquinone oxidoreductase activity in vitro using bovine heart electron transport particles (see Singer [31] for details).

The original library emphasizing bridge region **III** gave the IC_{50} values for **25–76** indicated in Figure 4 and the SAR summarized in Table 1. Compounds containing a conjugated and/or rigid bridging unit (i.e. chalcones, stilbenes, coumarins, heterocycles or alkynes) exhibited low activity ($IC_{50} > 1000$ nM) similar to those for most of the benzopyran-containing natural products (**11–15**, Figure 3). More interestingly, methylenes in the bridge unit, for greater conformational flexibility, resulted in higher activity dependent on the substituent pattern on the terminal aromatic ring, i.e. 220 nM IC_{50} for 3,4-dimethoxybenzyl esters **42** and 55 nM IC_{50} for 3,4,5-trimethoxybenzyl ester **55**, the most potent inhibitor in the screening library. The corresponding amides (**31** and **44**, Figure 4), presumably more polar than their ester counterparts, were significantly less active (40- and 10-fold, respectively), suggesting the possible importance of lipophilicity at region **III**.

The first of the focused libraries (**91–127**, Figure 5) exam-

Table 2
Selected data for growth inhibition (GI_{50}) of compounds 55, 158, 165 and 178 in NCI cancer cell lines[a].

Cancer cell type	GI_{50} (nM)				
	165	**158**	**178**	**55**	Average[b]
Leukemia					
HL-60	340	14	840	1810	750
K-562	730	1540	5090	2900	2800
MOLT-4	96	340	1230	6800	2560
RPMI-8226	940	3040	2660	4760	2850
NSC lung					
EKVX	66	680	3930	8620	3320
HOP-62	830	280	6690	31300	9780
NCI-H226	330	1090	5560	15500	5620
NCI-H322M	180	560	2210	49600	13100
Colon					
HCT-116	740	1370	4850	7930	3720
HCT-15	440	12600	3970	8940	6490
SW-620	660	23300	6400	21300	12900
CNS					
SF-295	690	23100	4580	23300	12900
SNB-19	660	17100	6110	11700	8890
U-251	210	430	2580	14300	4380
Melanoma					
LOX IMVI	180	19700	3050	9100	8010
MALME-3M	320	13400	2370	7700	5950
SK-MEL-5	490	1910	5160	3200	2690
UACC-257	210	780	3010	14500	4630
Breast					
MCF-7	3080	880	6570	9100	4910
NCI/ADR-RES	670	2500	2350	6800	3080
HS 578T	600	860	7400	25000	8470
MDA-MB-435	2790	37200	7110	14800	15500
Average[c]	690	7380	4300	13600	

[a]Assays were performed by the Developmental Therapeutics Program of the National Cancer Institute, USA. The compounds were provided as DMSO solutions and evaluated for their in vitro cytostatic properties against 60 human cell lines using the NCI standard protocol.
[b]Average GI_{50} value for compounds **55**, **158**, **165** and **178** in a particular cell line.
[c]Average GI_{50} value for a single compound in all cell lines.

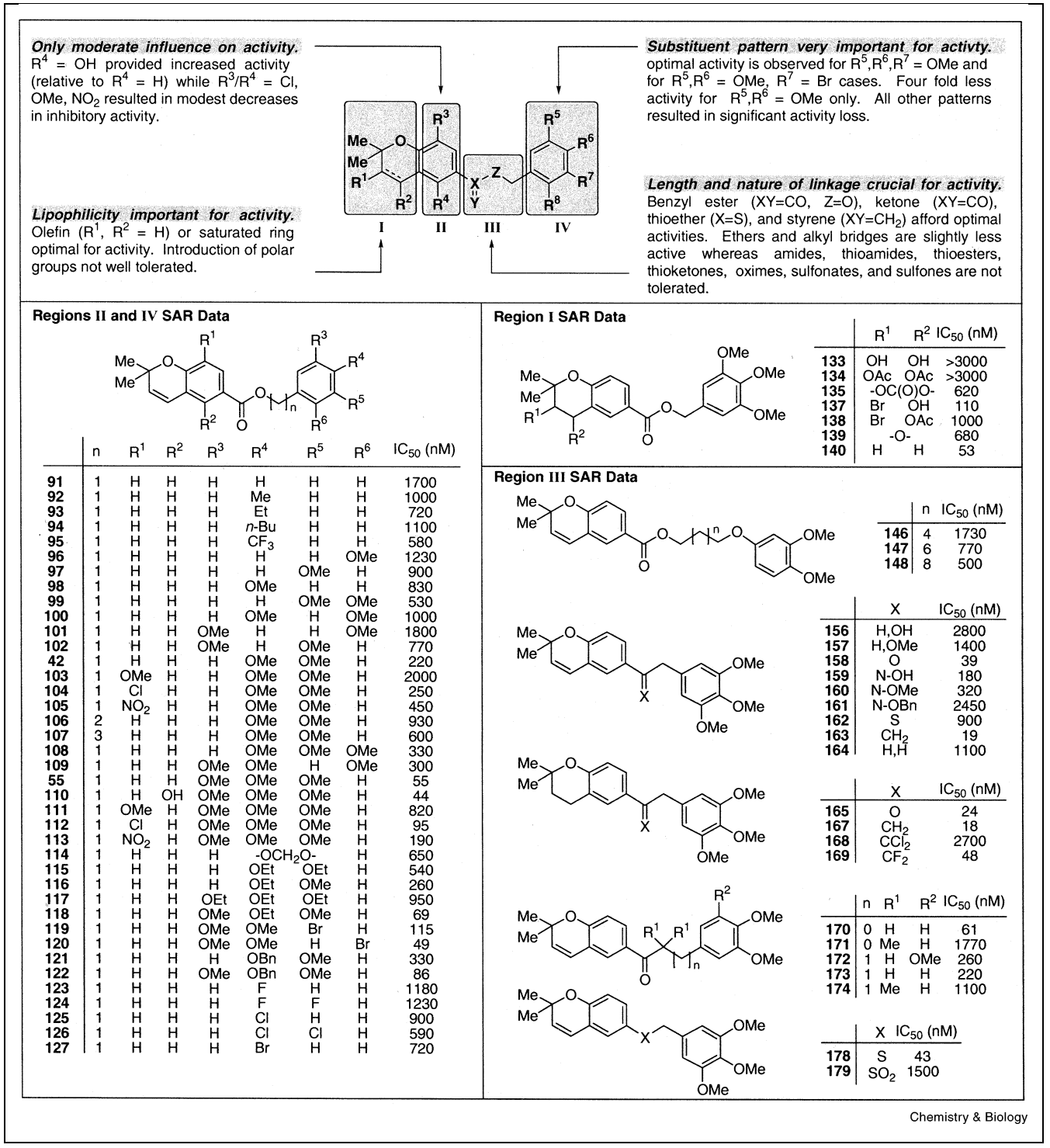

	n	R^1	R^2	R^3	R^4	R^5	R^6	IC_{50} (nM)
91	1	H	H	H	H	H	H	1700
92	1	H	H	H	Me	H	H	1000
93	1	H	H	H	Et	H	H	720
94	1	H	H	H	*n*-Bu	H	H	1100
95	1	H	H	H	CF_3	H	H	580
96	1	H	H	H	H	H	OMe	1230
97	1	H	H	H	H	OMe	H	900
98	1	H	H	H	OMe	H	H	830
99	1	H	H	H	H	OMe	OMe	530
100	1	H	H	H	OMe	H	OMe	1000
101	1	H	H	OMe	H	H	OMe	1800
102	1	H	H	OMe	H	OMe	H	770
42	1	H	H	H	OMe	OMe	H	220
103	1	OMe	H	H	OMe	OMe	H	2000
104	1	Cl	H	H	OMe	OMe	H	250
105	1	NO_2	H	H	OMe	OMe	H	450
106	2	H	H	H	OMe	OMe	H	930
107	3	H	H	H	OMe	OMe	H	600
108	1	H	H	H	OMe	OMe	OMe	330
109	1	H	H	OMe	OMe	H	OMe	300
55	1	H	H	OMe	OMe	OMe	H	55
110	1	H	OH	OMe	OMe	OMe	H	44
111	1	OMe	H	OMe	OMe	OMe	H	820
112	1	Cl	H	OMe	OMe	OMe	H	95
113	1	NO_2	H	OMe	OMe	OMe	H	190
114	1	H	H	H	$-OCH_2O-$		H	650
115	1	H	H	H	OEt	OEt	H	540
116	1	H	H	H	OEt	OMe	H	260
117	1	H	H	OEt	OEt	OEt	H	950
118	1	H	H	OMe	OEt	OMe	H	69
119	1	H	H	OMe	OMe	Br	H	115
120	1	H	H	OMe	OMe	H	Br	49
121	1	H	H	H	OBn	OMe	H	330
122	1	H	H	OMe	OBn	OMe	H	86
123	1	H	H	H	H	F	H	1180
124	1	H	H	H	F	F	H	1230
125	1	H	H	H	Cl	H	H	900
126	1	H	H	H	Cl	Cl	H	590
127	1	H	H	H	Br	H	H	720

	R^1	R^2	IC_{50} (nM)
133	OH	OH	>3000
134	OAc	OAc	>3000
135	$-OC(O)O-$		620
137	Br	OH	110
138	Br	OAc	1000
139	$-O-$		680
140	H	H	53

	n	IC_{50} (nM)
146	4	1730
147	6	770
148	8	500

	X	IC_{50} (nM)
156	H,OH	2800
157	H,OMe	1400
158	O	39
159	N-OH	180
160	N-OMe	320
161	N-OBn	2450
162	S	900
163	CH_2	19
164	H,H	1100

	X	IC_{50} (nM)
165	O	24
167	CH_2	18
168	CCl_2	2700
169	CF_2	48

	n	R^1	R^2	IC_{50} (nM)
170	0	H	H	61
171	0	Me	H	1770
172	1	H	OMe	260
173	1	H	H	220
174	1	Me	H	1100

	X	IC_{50} (nM)
178	S	43
179	SO_2	1500

Figure 5. Summary of structure activity trends observed for benzopyran-based inhibitors of NADH:ubiquinone oxidoreductase.

ined the substituent patterns for aromatic regions **II** and **IV**. Somewhat surprisingly, only esters **110** (IC_{50} = 44 nM) and **120** (IC_{50} = 49 nM) exhibited marginally improved activity over the original 3,4,5-trimethoxybenzyl ester **55** (IC_{50} = 55 nM). Varying substituents on the aromatic benzopyran ring only moderately influenced activity, e.g. introducing a halogen at R^1 (**42** → **104**; **55** → **112**) or a hydroxyl group at R^2 (**55** → **110**). A bulky substituent of the

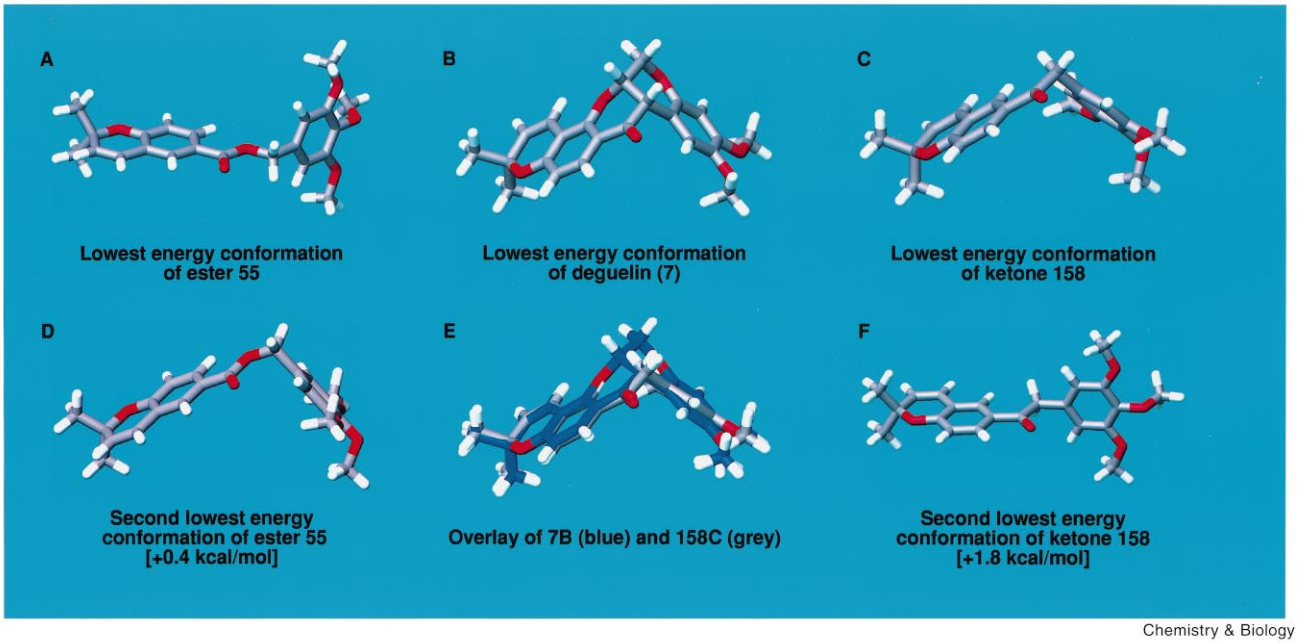

Figure 7. Molecular modeling of deguelin (**7**), ester **55**, and ketone **158**.

oxygen at R^4 (**42**→**121**; **55**→**122**) resulted in only slightly diminished inhibitory activity implying the greater importance of electronic rather than steric factors at this position. More generally, the 3,4,5-trimethoxyphenyl substituent is at or near the optimum for region **IV**.

The second focused library considered modifications of the pyran ring system (Figure 5). Introduction of a polar functionality on the pyran ring (i.e. **133** and **134**) significantly compromised activity, and less polar substituents (i.e. **135**–**139**) afforded no improvements. However, conversion to its saturated counterpart (**55**→**140**) resulted in a compound which retained potent biological activity (IC_{50} = 53 nM) yet was presumably metabolically more stable owing to the removal of the oxidatively sensitive pyran olefin.

A final focused library reexamined the bridging unit (region **III**) with keto-analogs revealing several interesting trends (Figure 5). First, ketone **158** was more active than the original ester lead with an IC_{50} value of 39 nM. Alcohol **156**, ether **157**, oximes **159**–**161**, thioketone **162**, and compound **164** were significantly less active than ketone **158**. Removal of the pyran olefin of ketone **158** via hydrogenation provided compound **165** which was almost twice as active as the parent olefin with an IC_{50} value of 24 nM. Intriguingly, conversion of the ketone to the corresponding olefin also increased activity as demonstrated for compound **163** (IC_{50} = 19 nM) and its saturated pyran counterpart **167** (IC_{50} = 18 nM). Substitution of the olefin protons with halogens (i.e. structures **168** and **169**) resulted in dichloro- and difluoro-analogs with reduced activity (IC_{50} values 2700 and 48 nM, respectively). On a separate note, thioether **178** was quite active with an IC_{50} of 43 nM, whereas the more polar sulfone **179** was inactive.

The overall results summarized in Figure 5 prompted selection of **55**, **158**, **163**, **165**, **167** and **178** (Figure 6) for further biological testing. Despite their structural simplicity, the inhibitory activity of these compounds approached that for the most potent natural product in this series, namely deguelin (**7**, Figure 3) with an IC_{50} value of 6.9 nM. Moreover, unlike the structurally complex deguelin, these lead compounds were simple to construct and thus could be readily modified to improve pharmacological properties, solubility or biostability.

The identified lead compounds were evaluated in several cell-based assays. The first involved determination of the cytotoxic concentrations (LC_{50} values) in MCF-7 human epithelial breast cancer cells using the MTT assay [16]. The six compounds tested showed low cytotoxicity in the MCF-7 cells (LC_{50} > 30000 nM). Secondly, compounds **55**, **158**, **165** and **178** were also evaluated in the NCI 60-cell cancer panel for the concentration leading to 50% growth inhibition (GI_{50}; see representative examples in Table 2) [32]. Moderate to good activity was observed in growth inhibition in various cell lines. The leukemia cells are generally the most sensitive (GI_{50} from 750 to 2850

nM) and the CNS cells the least sensitive (GI_{50} from 4380 to 12900 nM) to these compounds and the overall potency order is **165** > **178** > **158** > **55**. The combination of rather potent growth inhibition and possibly low cytotoxicity makes these compounds interesting lead structures as potential chemopreventive/chemotherapeutic agents.

Rationalization of SAR by molecular modeling

In an effort to better understand the molecular basis for the potent inhibitory activity exhibited by several of these compounds, molecular modeling studies were undertaken. Specifically, we hoped to compare the three-dimensional orientation of these leads to that of the structurally more complex natural product deguelin [7] (**7**, Figure 3) which remains the most potent compound in the benzopyran series. As illustrated in Figure 7, the semi-rigid structure of deguelin (**7**) was first minimized with molecular mechanics calculations (Insight II, CFF93 force field [33]) which provided its lowest energy conformation as the skewed structure denoted as **B** in Figure 7. Subsequently, ester **55** (Figure 6) and ketone **158** (Figure 6) were also minimized with the two lowest energy levels of each presented in Figure 7 (i.e. structures **A** and **D** for ester **55** and structures **C** and **F** for ketone **158**). Comparison of these minimized structures revealed that the second lowest energy conformation of ester **55** (structure **D**) and the lowest energy conformation of ketone **158** (structure **C**) resembled quite closely the bent configuration of deguelin **7** (structure **B**). In fact, the overlay of the lowest energy conformations of deguelin **7** (**B**) and ketone **158** (**C**), presented in diagram **E** (Figure 7), illustrate a strong homology between the two structures. The fact that the lowest energy configuration of ketone **158** best matched deguelin, whereas the less populated second lowest energy configuration of ester **55** matched deguelin was consistent with the fact that ketone **158** with an IC_{50} value of 39 nM was more potent than ester **55** which possessed an IC_{50} value of 55 nM.

Significance

Herein we have described how synthetic combinatorial libraries, modeled after natural products, can be utilized to discover novel and structurally simple lead compounds as inhibitors of the enzyme NADH:ubiquinone oxidoreductase (the current structure activity relationships complement previous work in the rotenone series; for a discussion see [34,35]). After discovery, several of these lead inhibitors were optimized through the synthesis of focused libraries which refined specific sub-units of the lead compounds. Ultimately a collection of benzopyran-based inhibitors with IC_{50} values 18–55 nM were identified. Several of these inhibitors were then evaluated in cell-based assays to evaluate their cytotoxic and cytostatic properties. Interestingly, while most of the compounds were relatively non-cytotoxic, several exhibit potent cytostatic activities across a variety of cancer types and cell lines. The ability of these small molecules to inhibit cancer cell growth, perhaps mediated by the ability to interrupt ODC activity, makes them potential candidates for further development as chemopreventive/chemotherapeutic agents. Further evaluation of these compounds is in progress along with the application of similar natural product-like combinatorial libraries to the discovery of lead compounds in other biological systems.

Acknowledgements

We would like to thank Dr. Ven Narayanan of the National Cancer Institute's Developmental Therapeutics Program for anticancer screening and Chris Boddy (TSRI) for assistance with molecular modeling. Financial support for this work at La Jolla was provided by The Skaggs Institute for Chemical Biology and the National Institutes of Health (USA), fellowships from the Department of Defense (to J.P.), the American Chemical Society Division of Medicinal Chemistry (sponsored by Parke-Davis, Hoechst Marion Roussel, Abbott, Wyeth Ayerst, and Bristol Myers Squibb) (to J.P.), and grants from CaPCURE Amgen, Bayer AG, Boehringer-Ingelheim, Glaxo, Hoffmann-La Roche, DuPont, Merck, Novartis, Pfizer, and Schering Plough. Support (to J.E.C.) also came from the William Muriece Hoskins Chair in Chemical and Molecular Entomology of the University of California at Berkeley.

References

1. Walker, J.E. (1992). The NADH:ubiquinone oxidoreductase (complex I) of respiratory chains. *Q. Rev. Biophys.* **25**, 253–324.
2. Ernster, L., Luft, R. & Orrenius, S. (1995). Mitochondrial Diseases, Nobel Symposium 90. *Biochim. Biophys. Acta* **1271**, 1–292.
3. Degli Esposti, M. (1998). Inhibitors of NADH-ubiquinone reductase: an overview. *Biochim. Biophys. Acta* **1364**, 222–235.
4. Barrientos, A. & Moraes, C.T. (1999). Titrating the effects of mitochondrial complex I impairment in the cell physiology. *J. Biol. Chem.* **274**, 16188–16197.
5. Schuler, F., Yano, Y., Bernado, S.D., Yagi, T., Van Kovskaya, V., Singer, T.P. & Casida, J.E. (1999). NADH-quinone oxidoreductase: PSST subunit couples electron transfer from iron–sulfur cluster N2 to quinone. *Proc. Natl. Acad. Sci. USA* **96**, 4149–4153.
6. Earley, F.G. & Ragan, C.I. (1984). Photoaffinity labeling of mitochondrial NADH dehydrogenase with arylazidoamorphigenin, an analogue of rotenone. *Biochem. J.* **224**, 525–534.
7. Earley, F.G., Patel, S.D., Ragan, C.I. & Attardi, G. (1987). Photolabelling of a mitochondrially encoded subunit of NADH dehydrogenase with [^{3}H]dihydrorotenone. *FEBS Lett.* **219**, 108–112.
8. Lümmen, P. (1998). Complex I inhibitors as insecticides and acaricides. *Biochim. Biophys. Acta* **1364**, 287–296.
9. Fang, N. & Casida, J.E. (1998). Anticancer action of cubé insecticide: Correlation for rotenoid constituents between inhibition of NADH:ubiquinone oxidoreductase and induced ornithine decarboxylase activities. *Proc. Natl. Acad. Sci. USA* **95**, 3380–3384.
10. Seiler, N., Atanassov, C.L. & Raul, F. (1998). Polyamine metabolism as target for cancer chemoprevention (review). *Int. J. Oncol.* **13**, 993–1006.
11. Udeani, G.O., Gerhäuser, C., Thomas, C.F., Moon, R.C., Kosmeder, J.W., Kinghorn, A.D., Moriarty, R.M. & Pezzuto, J.M. (1997). Cancer chemopreventive activity mediated by deguelin, a naturally occurring rotenoid. *Cancer Res.* **57**, 3424–3428.
12. Gerhäuser, C., Lee, S.K., Kosmeder, J.W., Moriarty, R.M., Hamel, E., Mehta, R.G., Moon, R.C. & Pezzuto, J.M. (1997). Regulation of ornithine decarboxylase induction by deguelin, a natural product cancer chemopreventive agent. *Cancer Res.* **57**, 3429–3435.
13. Gerhäuser, C., Mar, W., Lee, S.K., Suh, N., Luo, Y., Kosmeder, J., Luyengi, L., Fong, H.H.S., Kinghorn, A.D., Moriarty, R.M., Mehta, R.G., Constantino, A., Moon, R.C. & Pezzuto, J.M. (1995). Rotenoids mediate potent cancer chemopreventive activity through transcriptional regulation of ornithine decarboxylase. *Nat. Med.* **1**, 260–266.
14. Mills, K.I., Woodgate, L.J., Gilkes, A.F., Walsh, V., Sweeney, M.C., Brown, G. & Burnett, A.K. (1999). Inhibition of mitochondrial function in HL60 cells is associated with an increased apoptosis and expression of CD14. *Biochem. Biophys. Res. Commun.* **263**, 294–300.

15. Fang, N. & Casida, J.E. (1999). New bioactive flavanoids and stilbenes in Cubé resin insecticide. *J. Nat. Prod.* **62**, 205–210.
16. Fang, N., Rowlands, J.C. & Casida, J.E. (1997). Anomalous structure-activity relationships of 13-*homo*-13-oxarotenoids and 13-*homo*-13-oxadehydrorotenoids. *Chem. Res. Toxicol.* **10**, 853–858.
17. Nicolaou, K.C., Pfefferkorn, J.A., Roecker, A.J., Cao, G.-Q., Barluenga, S. & Mitchell, H.J. (2000). Natural product-like libraries based on privileged structures I: General principles and solid phase synthesis of benzopyrans. *J. Am. Chem. Soc.* **122**, 9939–9953.
18. Nicolaou, K.C., Pfefferkorn, J.A., Mitchell, H.J., Roecker, A.J., Barluenga, S. & Cao, G.-Q. (2000). Natural product-like libraries based on privileged structures II: Construction of a 10 000-membered benzopyran library by directed sorting split-and-pool chemistry using NanoKans™ and optical encoding. *J. Am. Chem. Soc.* **122**, 9953–9967.
19. Nicolaou, K.C., Pfefferkorn, J.A., Barluenga, S., Mitchell, H.J., Roecker, A.J. & Cao, G.-Q. (2000). Natural product-like libraries based on privileged structures III: The 'libraries from libraries' principle for diversity enhancement of benzopyran libraries. *J. Am. Chem. Soc.* **122**, 9968–9976.
20. Nicolaou, K.C., Pfefferkorn, J.A. & Cao, G.-Q. (2000). Selenium-based solid phase synthesis of benzopyrans I: Applications to combinatorial synthesis of natural products. *Angew. Chem. Int. Ed.* **39**, 734–739.
21. Nicolaou, K.C., Cao, G.-Q. & Pfefferkorn, J.A. (2000). Selenium-based solid phase synthesis of benzopyrans II: Applications to combinatorial synthesis of medicinally relevant small organic molecules. *Angew. Chem. Int. Ed.* **39**, 739–743.
22. Nicolaou, K.C., Pastor, J., Barluenga, S. & Winssinger, N. (1998). Polymer-supported selenium reagents for organic synthesis. *Chem. Commun.*, 1947–1948.
23. Bell, D., Davies, M.R., Geen, G.R. & Mann, I.S. (1995). *Synthesis*, 707–712.
24. Fenwick, A.E. (1993). The synthesis of 2,2-bis(trifluoromethyl)benzopyran derivatives: A new route to an important class of potassium channel activators. *Tetrahedron Lett.* **34**, 1815–1818.
25. Gabbutt, C.D., Hepworth, J.D., Heron, B.M. & Rahman, M.M. (1994). Allenes from 3-bromo-*2H*-1-benzopyrans. *J. Chem. Soc. Perkin Trans.* **I**, 1733–1737.
26. Buckle, D.R., Arch, J.R.S., Fenwick, A.E., Houge-Frydrych, S.V., Pinto, I.L., Smith, D.G., Taylor, S.G. & Tedder, J.M. (1990). Relaxant activity of 4-amido-3,4-dihydro-*2H*-1-benzopyran-3-ol and 4-amido-*2H*-1-benzopyrans on guinea pig isolated trachealis. *J. Med. Chem.* **33**, 3028–3034.
27. Ding, C.Z. (1996). A convenient synthesis of 6-substituted-2,2-dimethyl-*2H*-1-benzopyrans. *Syn. Commun.* **26**, 4267–4273.
28. Clement, B.A. & Soulen, R.L. (1974). Reaction of a phosphorus ylide with aliphatic acyl cyanides. *J. Org. Chem.* **39**, 97–98.
29. Piettre, S.R. & Cabanas, L. (1996). Reinvestigation of the Wadsworth–Emmons reaction involving lithium difluromethylenephosphonate. *Tetrahedron Lett.* **37**, 5881–5884.
30. Sato, M., Goto, J., Yamana, Y., Chiba, Y., Jinno, S., Satake, S. & Iwata, C. (1995). Synthesis and evaluation of novel fluorinated sulotroban-related sulfonamide derivatives as thromboxane A_2 receptor antagonists. *Eur. J. Med. Chem.* **30**, 403–414.
31. Singer, T.P. (1974). Determination of the activity of succinate, NADH, choline, and a glycerophosphate dehydrogenases. In *Methods of Biochemical Analysis*. (Glick, D., ed.), 22, pp. 123–175, Wiley, New York.
32. Monks, A., Scudiero, D., Skehan, P., Shoemaker, R., Paull, K., Vistica, D., Hose, C., Langley, J., Cronise, P., Vaigro-Wolff, A., Gray-Goodrich, M., Campbell, H., Mayo, J. & Boyd, M. (1991). Feasibility of a high-flux anticancer drug screen using a diverse panel of cultured human tumor cell lines. *J. Natl. Cancer Inst.* **83**, 757–766.
33. Hwang, M.J., Stockfisch, T.P. & Hagler, A.T. (1994). Derivation of class II force fields. 2. Derivation and characterization of a class II force field, CFF93, for the alkyl functional group and alkane molecules. *J. Am. Chem. Soc.* **116**, 2515–2525.
34. Crombie, L., Josephs, J.L., Cayley, J., Larkin, J. & Weston, J.B. (1992). The rotenoid core structure: modifications to define the requirements of the toxophore. *Bioorg. Med. Chem. Lett.* **1**, 13–16.
35. Levett, P.C., Whiting, D.A., Cayley, J., Cockerill, G.S. & Weston, J.B. (1994). Structural requirements for respiratory inhibition by rotenoids: is an intact B/C ring system essential? *Bioorg. Med. Chem. Lett.* **3**, 505–508.